LIGHT-SCATTERING STUDIES OF BULL SPERMATOZOA

II. Interaction and Concentration Effects

M. W. WOOLFORD
Ruakura Agricultural Research Center Hamilton, New Zealand

J. D. HARVEY
Physics Department, The University of Auckland, Private Bag, Auckland. New Zealand

ABSTRACT The complete autocorrelation function of the intensity fluctuations of laser light scattered from motile bull spermatozoa is shown to depend upon several factors not previously considered. Samples of bull spermatozoa generally contain a substantial proportion of dead cells, which give rise to slowly decaying components of the autocorrelation function. Whereas previous work has concentrated on the form of the fast decaying autocorrelation component, we are concerned here with the relative amplitude and shape of the slow autocorrelation component and the general form of the composite function. In principle, the relative amplitudes of the fast and slow components of the autocorrelation function can be used as an assay of the proportion of swimming cells. We show that this amplitude ratio depends upon cell concentration, scattering cell geometry, and scattering angle. A simple model is developed to explain these results on the basis of the asymmetry of light scattered from these cells, motile/immotile cell interactions, wall-swimming effects, and geotactic reorientation of dead cells.

INTRODUCTION

A series of papers has appeared in the last decade describing the scattering of laser light from motile spermatozoa (see Harvey and Woolford, 1980 and references therein). The majority of these studies have taken spermatozoa to behave as Doppler point sources, and the spectrum or autocorrelation function of the scattered light has been analysed accordingly. It has recently been shown for bull spermatozoa, however, (Craig et al., 1979; Harvey and Woolford, 1980) that such a treatment is quite inappropriate, the spectrum of the photocurrent fluctuations being dominated, not by Doppler effects associated with the translational motion, but by intensity fluctuations associated with the rotational motions of the head. Such fluctuations arise from a particular head shape for the bull spermatozoon which may be modeled as a leaf-shaped mirror rotating about the translation vector (Harvey and Woolford, 1980). Substantial intensity peaks at the detector, generated by specular reflection, occur when the translation vector lies closely perpendicular to the scattering vector. These extremely large intensity fluctuations generated by the head rotation mask any Doppler beat component due to center of mass motion in the detected optical field.

Most published work has studied the spectrum of light scattered from motile cells. Nearly all fresh samples of mammalian spermatozoa, however, contain a significant proportion of immotile cells, the characterization of which is often of considerable importance in artifical breeding. Previous interpretations of laser light scattering data have generally assumed that immotile spermatozoa behave as independent diffusing Brownian scatterers that contribute a slowly decaying component to the autocorrelation function of the scattered field (Cummins, 1977, and references therein). Under such conditions, the argument of Nossal (1971) may be applied wherein the proportion of immotile scatterers may be determined by fitting the two components of the observed autocorrelation function. Subsequent workers (Hallett et al., 1978), recognizing the inadequacy of this model, considered that an additional component was required to take account of defective or circular swimmers and fitted their autocorrelation data as three component functions, with the component from dead cells represented by a fourth order polynomial. It is important to ascertain whether such approaches are valid, and whether they can be used to determine the proportion of immotile cells, since this is one of the most useful parameters of sperm motility to determine in artificial breeding studies.

Our results show that previous interpretations of the immotile (or slow) component have been simplistic and that a complete understanding of the composite autocorrelation function generated by a mixture of motile and immotile cells requires consideration of the particular shape of the bull spermatozoon, spatial orientation effects, the distribution of spermatozoa within the scattering cell, and interactions or collisions between motile and immotile cells.

Autocorrelation Functions Generated by Mixtures of Motile and Immotile Bull Spermatozoa

The simplest way in which to treat the light scattered from a mixture of motile and immotile cells is to express the autocorrelation function as

$$g^{(1)}(\tau) = F_M(\tau) + F_I(\tau), \tag{1}$$

where F_M and F_I are the autocorrelation functions of light scattered from motile and immotile fractions. The explicit form of both autocorrelation components depends on the kinetic models appropriate to the two fractions. If it is assumed that the scattered field is generated in the same way for both motile and immotile cells, then the first order autocorrelation function may be expressed as

$$g^{(1)}(\tau) = \epsilon f_i(\tau) + (1 - \epsilon) f_m(\tau), \tag{2}$$

where $\epsilon = \rho_i/(\rho_i + \rho_m)$ is the proportion of immotile cells in the suspension, ρ_m and ρ_i being the concentrations within the scattering volume of motile and immotile cells, respectively.

If $f_m(\tau)$ is taken to result from the Doppler beat spectrum generated by an assembly of moving point scatterers and $f_i(\tau)$ to arise from Brownian diffusion of the immotile scatterers, ϵ gives an absolute measurement of the fraction immotile if interaction effects between the two fractions are neglected.

Recent work (see Craig et al., 1979; and Harvey and Woolford, 1980), however, has shown that $f_m(\tau)$ results from intensity fluctuations as the head of the swimming spermatozoon rotates, giving an autocorrelation function that depends on the details of the swimming motion. In particular, the autocorrelation function of the optical field generated by a single rotating spermatozoon may be evaluated analytically at a point in the far-field if spermatozoa are modeled as ellipsoidal particles and the Rayleigh-Gans approximation is used. The scattered intensity at the detector peaks when the normal to the rotating head plane lies along the scattering vector and (at a scattering angle of 20°) has a width of ~20° at half-intensity (Woolford, 1981). As a consequence of this peaked scattering lobe, motile cells only become visible to the detector when the translation axis falls within ±20° of the perpendicular to the scattering vector. Consequently the detector receives significant light from only a fraction of the motile cells, and the results reported earlier (Harvey and Woolford, 1980) show that this fraction will depend on the scattering angle and on the dimensions and shape of the model assumed for the sperm head. Photographic measurements indicate that only ~20% of the motile population contributes to the amplitude of the motile autocorrelation component $F_M(\tau)$.

The same orientation effects are observed for dead spermatozoa (Harvey and Woolford, 1980) but additional complications arise from the distribution of axial orientations which, through geotaxis, become strongly peaked in the "head-down" position. This arises from the relatively high density of the bull sperm head compared with that of the flagellum. It has been shown (Roberts, 1970, 1972) that the rate of geotactic relaxation towards the head-down position may be expressed by

$$\frac{d\phi}{dt} = \beta \sin \phi, \tag{3}$$

where ϕ is the angle between the longitudinal axis of the spermatozoon and the vertical.

An immediate consequence of geotaxis and the previously described orientational effect (Harvey and Woolford, 1980) on the scattered light is that dead cells orient to a head-down attitude and therefore become visible to a detector aligned at forward scattering angles in the horizontal plane but invisible to a detector aligned at the same scattering angle in the vertical plane. The time dependence of the geotactic effect in 100% immotile suspensions has been shown (Harvey and Woolford, 1980) to be consistent with the geotactic reorientation rate expected from Eq. 3. The light scattered to the detector by isotropically swimming motile cells, however, is the same for both planes of detector alignment.

It is important to note that, at any instant, only a small proportion of a population of dead sedimenting cells, in a head-down attitude, will be favorably oriented to reflect light from the laser to the detector, but that the time averaged intensity of the light from a slowly rotating sedimenting cell will be the same as that from a fast spinning cell swimming vertically. Even in the absence of rotational motion of the dead cells, the ensemble averaged intensity from a randomly oriented population of dead cells in the head-down attitude will be the same as that from the same number of fast spinning cells that are swimming vertically and spinning about this axis. For this reason, the term "visible" is used to describe all dead cells sedimenting vertically when a detector is oriented in the horizontal plane, even though not all of the cells will be reflecting light to the detector at any given time.

These effects may be accounted for in Eq. 2 by introducing factors which adjust the amplitudes of two correlation functions arising from motile and immotile cells, appropriately, hence

$$g^{(1)}(\tau) = \epsilon A f_i(\tau) + (1 - \epsilon) B f_m(\tau), \tag{4}$$

where A is the fraction of the immotile population visible to the detector and B is the corresponding fraction of motile cells. The fraction A will be time dependent after sample insertion, until geotactic relaxation is complete. Over the geotactic relaxation time, it may be expected that A will tend to 1 for a horizontally aligned detector, and to zero for a vertically aligned detector (Harvey and Woolford, 1980). In addition, for any plane of orientation of the detector, the ratio A/B and hence the relative amplitudes of the two

correlation components at $\tau = 0$ will be scattering angle dependent. Such a simple modification to Eq. 2, however, predicts no concentration dependence in the relative amplitudes of the two components.

A further important factor which needs to be considered, in view of the large optical asymetry of the immotile population, concerns the interactions between the two fractions. Interactive or cooperative effects between spermatozoa are well known at high concentration (Walton, 1952) and interactions between swimming cells have been observed at concentrations typical of light scattering experiments (Rothschild, 1963*a*; van Duijn, 1973). Such interactions may result in an increased broadening of the distribution of immotile cell orientations about the vertical head-down attitude and so introduce a concentration dependent factor into the coefficient A of Eq. 4. For example, an immotile bull spermatozoon initially in a head-down attitude is visible to a horizontally aligned detector (in the sense explained previously). However, should the cell experience a perturbation by a passing motile cell, it may become reoriented to an attitude or tilt angle outside the range of visibility and thereafter geotactically relax back towards the vertical at a rate consistent with that of Eq. 3. An increasing concentration of motile spermatozoa results in an approach towards an isotropic distribution of immotile cell orientations, in which case A approaches B in Eq. 4, and in the limit, a similar proportion of motile and immotile cells becomes visible to both horizontally and vertically aligned detectors, and the correlation function may be satisfactorily described by Eq. 2. At such concentrations, however, interactions between cells are so frequent that the two components of the autocorrelation function have similar decay times and are difficult to separate.

A further kinetic effect within samples of bull spermatozoa that needs to be accounted for is the pronounced tendency of motile cells to accumulate on the internal surface of a glass cuvette. This phenomenon has been studied previously (Katz and Blake, 1974; Rothschild, 1963*b*) and arises from the inability of cells which swim onto a smooth surface to develop a propulsive component normal to the surface (other than through collisions with other cells). As a consequence of this phenomenon, particularly at lower sample concentrations ($<10^7$ sperm/ml), an initially homogeneous distribution of motile and immotile cells at the time of sample injection rapidly becomes heterogeneous, with a significantly higher concentration of motile cells to be found on the internal surfaces of the cuvette although the immotile cells remain uniformly distributed throughout the sample cell. Clearly, under these conditions the coefficient B in Eq. 4 will depend on the specific location of the scattering volume within the sample chamber and the geometry and volume of the cuvette.

It is apparent, therefore that a detailed description of this relatively complex system of interacting mixtures of large-structured scattering centers requires quantitative details of collisional interactions, swimming motions, and wall-swimming effects which are not currently available. We consider that a full theoretical treatment of the scattered-light field from this system is not a feasible or profitable undertaking at this time. We present here experimental results concerning the full autocorrelation function of the scattered intensity that indicate the complexity of the problem and the many influences on the scattered light intensity. It is useful, however, to attempt to identify some general features of these correlation functions, which, it may be expected, are largely insensitive to the details of any models for the kinetic behavior of the live and dead fractions. Our experimental results provide strong evidence for the importance of interactions between live and dead components of the mixtures, and we consider that the general form of the autocorrelation function and the ratio of the amplitudes of the live and dead components at forward angles can be understood on the basis of a simple interaction model.

The Fast Autocorrelation Component

Detailed calculations of the form of the function $f_m(\tau)$ are feasible using realistic swimming models, and calculations of this type have been reported by Craig et al. (1979), who found that the form of this part of the correlation function is determined by the rotational motion of the cell head. This result is to be expected on the basis of the results reported by Harvey and Woolford (1980), in which it was demonstrated that the swimming spermatozoa behave as spinning mirrors that only flash or reflect light to the detector when traveling in a direction close to the normal to the scattering vector, and thus contribute no significant Doppler shift to the scattered light. Using the Rayleigh-Gans-Debye approximation, the scattering amplitude for an ellipsoidal particle is proportional to $J_{3/2}[k\sigma(t)]$, where $\sigma(t)$ is the perpendicular distance from the center of the particle to the tangent plane that is perpendicular to the scattering vector k at time t (see Harvey and Woolford, 1980). Thus, for rectilinear motion a thin spinning ellipsoid yields a correlation function of the form

$$g^{(1)}(\tau) = \langle E(t)E^*(t+\tau)\rangle \propto \langle e^{i\mathbf{k}\cdot\mathbf{v}\tau} J_{3/2}[k\sigma(t)]\, J_{3/2}[k\sigma(t+\tau)]\rangle. \quad (5)$$

This expression may be evaluated readily, using the approximation that $\mathbf{k} \cdot \mathbf{v}$ is zero (i.e., neglecting Doppler effects).

We have performed calculations of this type and have obtained results that are very similar to those obtained in the more extensive models of Craig et al. (1979), where helical motion of the center of mass is included. Such calculations are not needed, however, to interpret the autocorrelation functions that are our subject here, because these are collected using sample times that are of the same order as the decay time of the fast autocorrelation

component. The important parameter of the fast component in the context of these results is its amplitude at zero delay time when compared with that of the slow component.

The Slow Autocorrelation Component

The correlation function from a sample of immotile (100% dead) cells has a slow decay time (of the order of seconds) at forward scattering angles and exhibits no fast component. The slow component from a mixed sample of motile and immotile cells might be expected to have the same functional form as that of a 100% dead sample at the same concentration. Experimental investigation, however, shows that this is not the case. For a horizontally oriented detector, all cells in a 100% dead sample ultimately reach a (visible) head-down attitude via sedimentation, and the function is thus generated by the slow rotation or tumbling motion of the sedimenting cells with a possible contribution from rotational diffusion of the head about the long axis of the cell. In our experiments, this function was found to be nonexponential in the form, but approached single exponential behavior at small forward scattering angles ($<10°$). In all cases, however, the autocorrelation function decayed at a much slower rate for 100% dead cells than did the slow part of the correlation function from a mixture of motile and immotile cells. The decay rate of the slow component in a mixture was found to depend strongly on the vigor and concentration of the swimming fraction.

On the basis of these experiments, we conclude that a dominant influence on the form of the slow correlation function component at forward scattering angles is the perturbation of their slow sedimentation by interactions with motile cells.

If the probability of such an interaction per unit time is λ, then in time t the probability of a dead cell not being perturbed by a live cell is

$$P(t) = \lim_{\Delta t \to o.} (1 - \lambda \Delta t)^{t/\Delta t} = e^{-\lambda t}. \tag{6}$$

If it is further assumed that only those cells in a head-down attitude contribute to the slow correlation component (see Harvey and Woolford, 1980) and that a collision with a swimming cell reorients the cell to a new attitude from which the light scattered to the detector is negligible, then the slow correlation component may be evaluated by noting that the product $[E(t)E^*(t + \tau)]$ for the electric field scattered from a dead cell in a mixture is equal to zero if a collision occurs in time τ, or to that from a cell in a totally immotile sample if a collision does not occur, thus

$$\begin{aligned} f_i(\tau) &\propto \langle E_i(t)\, E_i^*(t+\tau) \rangle \\ &= \langle E_d(t)\, E_d^*(t+\tau)\, P(\tau) \rangle \\ &= P(\tau)\, f_d(\tau), \end{aligned} \tag{7}$$

where $f_d(\tau)$ is the correlation function from 100% dead cells and E_i and E_d represent the scattered electric field from immotile cells in a live/dead mixture and those in a 100% dead sample, respectively. If $f_d(\tau)$ has a very slow decay compared with $f_i(\tau)$ (i.e., $f_i(\tau) \approx$ const. over the time λ^{-1}) then the functional form of $f_i(\tau)$ will be given by

$$f_i(\tau) \approx e^{-\lambda \tau}. \tag{8}$$

Thus the effect of strong interactions is to produce an exponentially decaying correlation function whose decay constant is independent of scattering angle. Alternatively, at low scattering angles where $f_d(\tau)$ is found experimentally to approach a single exponential behavior ($f_d(\tau) \approx e^{-\gamma \tau}$), then

$$f_i(\tau) \approx e^{-(\lambda+\gamma)\tau}. \tag{9}$$

The decay rate λ is a function of the concentration and vigor of the motile cells, and may be related to the swimming parameters of the motile fraction by assuming that a swimming cell moves rectilinearly and perturbs all cells within a cylinder of radius r whose axis is the swimming trajectory. Then in time Δt,

$$\lambda \Delta t = N_m(\pi r^2 \bar{v} \Delta t)/V,$$

where $\bar{v}$ is the mean velocity of the swimming cell, V is the total volume of the cuvette, and N_m is the total number of motile cells in the cuvette

$$\therefore\ \lambda = \pi r^2 \bar{v} C, \tag{10}$$

where C is the concentration of motile cells. This simple theory thus also predicts that the decay constant of the slow component of the correlation function will be a linear function of the concentration of motile cells.

The Amplitude Ratio of the Fast and Slow Components

The ratio of the amplitudes of the fast and the slow autocorrelation components (referred to here as the autocorrelation amplitude ratio [AAR]) varies dramatically as a function of motile cell concentration. To obtain a complete quantitative explanation of this variation, it is necessary to provide an exact description of the various phenomena that are responsible. These phenomena include geotactic reorientation of the dead cells, optical anisotropy of the scattered-light field, details of the swimming motion and interactions between motile and immotile cells. An exact treatment is thus not a feasible undertaking at this time. It is possible, however, to develop a simplified model of the processes involved that gives a qualitative understanding of the light-scattering data (Woolford, 1981). This model assumes that collisions between motile and immotile cells are the dominant influence on the scattered intensity, as these collisions may reorient immotile cells away from the head-down attitude, in which they are visible to the detector, to another at which they are invisible. To see the significance of such collisions in a

typical light-scattering experiment, it is useful to estimate the collision frequency. The total interaction volume traced out by swimming cells in a time Δt within unit volume of the glass cuvette is given by $V_i = \pi r^2 \rho_m (1 - W)\, \bar{v} \Delta t = \lambda \Delta t$, where W is the fixed proportion of the motile cells which swim in the walls, and ρ_m is the total motile cell concentration. As a numerical example, assuming $W = 0.2$, $r = 50$ μm, $\bar{v} = 150$ μs^{-1}, and a motile cell concentration of only 10^6/ ml, this equation gives $\lambda = 0.94$ and thus a high probability of an immotile cell suffering a collision in 1 s (a typical decay time for the autocorrelation function of light scattered from a sample of 100% dead cells at forward angles).

The attitude or tilt angle of a cell (α) may be defined as the angle which the long axis of the cell makes with the vertical. To evaluate the mean intensity of the light scattered from the immotile cells, it is necessary to know the equilibrium distribution of the cells as a function of tilt angle, and the mean intensity of light scattered by the cells as a function of α. While the latter has been investigated using the Rayleigh-Gans-Debye approximation (see Harvey and Woolford, 1980), the former depends upon details of the interaction process which are not available. A much simplified approach has been developed elsewhere (Woolford, 1981), in which the equilibrium number of visible cells is estimated taking account of geotaxis and collisional redistribution of the cells.

The predictions of this model are in qualitative agreement with the data. In particular, the limiting values of the AAR as a function of concentration can be derived quite simply. At very low motile cell concentrations, interactions become negligible, all immotile cells become visible to a detector in the horizontal plane, and the AAR reduces

$$\lim_{C \to \infty} \mathrm{AAR} = \rho_i / [\rho_i + (1 - W)\gamma \rho_m], \qquad (11)$$

where γ is the proportion of swimming cells which are visible to the detector (at forward scattering angles γ will be of the order of 0.2: see Harvey and Woolford, 1980). At very high concentrations, interactions are so frequent that immotile cells become uniformly distributed with respect to tilt angle and

$$\lim_{C \to \infty} \mathrm{AAR} = \rho_i / [\rho_i + (1 - W)\rho_m]. \qquad (12)$$

If collisions are also so frequent that the cells become uniformly distributed throughout the scattering cuvette, then $W \to 0$ and this reduces to the proportion of dead cells, which is the value obtained in treatments which ignore the anisotropy of the cells and the wall-swimming effect. The smooth transition between these limits can be expected to occur at a concentration such that the immotile cells have a significant probability of being perturbed in a time characterized by the geotactic relaxation rate. This time is of the order of tens of seconds (see Harvey and Woolford, 1980 and Eq. 3) and thus the equilibrium distribution of dead cells, which is normally strongly peaked in the head-down direction, will be broadened sufficiently to affect the mean scattered intensity in the horizontal plane, if the collision probability λ is greater than about 0.1. Using the model developed in the previous section, this value of the interaction probability will be attained at a concentration between 10^5 and 10^6 cells depending on the value chosen for the interaction radius. It is likely that a perturbation sufficiently strong to reorient the attitude or tilt angle of the cell can only be caused by a direct collision with the head of a motile cell corresponding to an interaction radius of $\sim 5 \to 10$ μm. Under these conditions the AAR will be strongly affected by the concentration of motile cells in the region of 10^6 cells/ml. This interaction model thus predicts that the AAR will vary between two limits as the concentration of motile cells is increased. The total cell concentrations over which the AAR varies most strongly will of course depend upon the proportion of live cells.

EXPERIMENTAL METHODS

The light scattering apparatus employed in these studies was of similar design and geometry to that generally described by previous workers. The scattered light from samples of spermatozoa was collected at small forward scattering angles (generally <20°) by a lens of aperture 1 mm which formed a real inverted image of light scattered in the sample, on a screen located at twice the focal length of the lens. Such a system (Chu, 1974) allowed light to be collected from any desired location within the illuminated region of the sample by appropriately locating the phototube (Phillips 56AVP) aperture on the image when viewed through a microscope eye-piece.

The photodetector system was oriented at forward scattering angles in both the horizontal and vertical scattering planes for various experimental studies. Typically the laser beam was focussed to a diameter in the range 0.5–1 mm within the sample. This beam (488 nm from an argon-ion laser) was reduced to the order of 5–20 mW so as to minimize any irradiation effects on the sample.

Sample chambers of three basic designs were evaluated during the course of experimental studies (Woolford, 1981). Initial work used a simple open top glass spectrophotometer cell of path length 10 mm partially immersed in a temperature controlled water bath. Subsequently, problems with hydrodynamic stability of the suspending medium led to the development of a totally enclosed sample chamber having a depth of 2 mm and a path length of 10 mm fully immersed in a temperature controlled water-jacket. A third design used a short path length (1–2 mm), but was of greater depth (10 mm), as such depth was found necessary to take account of sedimentation of immotile cells and wall-swimming of the motile component. Thermal regulation of the sample chamber (normally at 37°C) within close limits (< ±0.05°C) over the signal sampling interval was essential to prevent convective motion of immotile cells, which may distort the functional form of the slow autocorrelation component.

The photodetector output signal, after amplification, was analysed by a 100 channel autocorrelator (Hewlett-Packard 3721A; Hewlett-Packard Co., Palo Alto, CA) with curve-fitting and other data handling being executed by an interfaced minicomputer (Computer Automation LSI 2-20G Computer Automation Co., Irvine, CA).

Samples

Our results were obtained using bull spermatozoa collected and processed by the New Zealand Dairy Board (Newstead Artificial Breeding Research Centre, Hamilton, New Zealand.). After collection from high

fertility bulls, samples were diluted to a holding concentration of typically 10^8 sperm/ml, in "Caprogen," an extender developed for artificial breeding service with liquid semen (Shannon, 1973) and having, as a base, sodium citrate–buffered egg yolk (EY). After prefiltering, the extender was optically cleared through solubilization with a 2% sodium citrate–based buffer to give a final 5% EY concentration and then passed through a 0.22-μm filter immediately before use.

Samples were generally found to be highly motile for 3–4 d if stored at $\sim 10^8$ sperm/ml in 5% Caprogen extender at 20°C. Normally experiments were carried out within 24 h of sperm collection, samples being prepared by further diluting from the holding concentration a few minutes before use. Freshly prepared and filtered EY extender was found to generate no significant background scattering (typically <1%) for low scattering angles (<20°) and concentrations up to the 5% level. The scattered intensity from the spermatozoa is strongly peaked in the forward direction, whereas the small background signal scattered from buffer diluted EY extender was more nearly isotropic. In consequence, at large scattering angles the signal from a protein aggregate component in the EY extender became significant in comparison with that from the spermatozoa. All experiments were thus carried out at forward scattering angles, using bull spermatozoa at concentrations in the range 0.25–10.0 × 10^6/ml in a 0.25% filtered EY extender where the signal from the buffer was negligible.

The ratio of motile/immotile spermatozoa in the suspension was adjusted by appropriate additions of dead cells to samples having a known proportion of dead cells in the raw semen, as determined by a nigrosin-eosin differential stain count immediately after collection. Toxic effects of added dead sperm (Shannon, 1965) were found not to be significant over the short timescale (<10 min) of sample preparation and autocorrelation data collection. To avoid possible problems with degradation of the sample in the cuvette, each autocorrelation function was derived from light scattered from a freshly diluted sample.

Data Processing

In these particular studies it was not necessary to characterize the signal generated by the motile fraction other than by its amplitude F_m (0). Therefore, in contrast with other reported work, autocorrelation was carried out at relatively long dwell times (generally 10 ms/ch) to allow the amplitude and functional form of the slow autocorrelation component $F_i(\tau)$ and the true baseline to be well defined. The low signal frequencies associated with the immotile fraction required lengthy data collection times to achieve satisfactory autocorrelation statistics. All functions were derived from 16,000–64,000 samples of the signal taken by the autocorrelator. The correlator was started after a standard equilibration time of 6 min had elapsed after sample insertion to allow for thermal equilibration and geotactic relaxation of the dead cells.

Fitting to the autocorrelation data was carried out by an iterative linearizing least-squares algorithm which fitted an exponential to the slowly decaying component $F_i(\tau)$ to obtain its amplitude, decay constant, and baseline. This enabled the AAR of the two components to be determined. The fitting range avoided the first ten channels (i.e., $\Delta\tau < 100$ ms) where $F_m(\tau)$ and $F_i(\tau)$ overlapped, the general features of such functions being shown in Fig. 1.

EXPERIMENTAL RESULTS

We have found the relationship between the percent motile cells and the light-scattering AAR as determined from computer fits to be markedly dependent on the sperm concentration. The data of Fig. 2 clearly show an increasing relative contribution from the immotile fraction with decreasing sperm concentration.

In attempting to understand the origin of the results displayed in Fig. 2 several possible explanations were considered. The number of cells in the scattering volume at

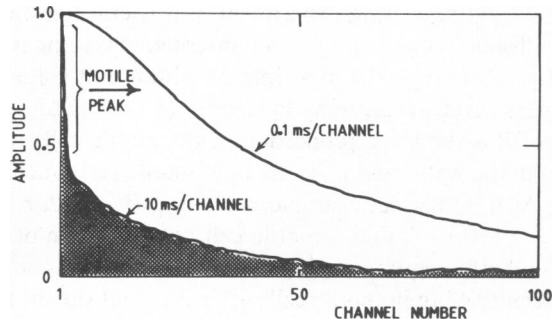

FIGURE 1 General features of the long timescale composite autocorrelation function (10 ms/ch) of the scattered intensity from a mixture of motile and immotile sperm cells. The fast decaying autocorrelation function (0.1 ms/ch) from the motile fraction is also shown illustrating the substantial difference in the decay time of the two components (k = 2.3 μm^{-1}, sample concentration 2 × 10^6 cells/ml).

any time (N_0) is not very large (possibly $<10^2$), and an experiment was performed to determine whether the AAR was dependent upon scattering volume size at a concentration of 10^6 sperm/ml. No such dependence was found over the population range $100 < N_0 < 2{,}000$, and we exclude the possibility that the slowly decaying autocorrelation component arose from intensity fluctuations created by variations in the scattering volume population.

Experiments performed with many different samples and concentrations, at various temperatures and scattering angles all suggested that the major influence on the amplitude and shape of $F_i(\tau)$ was the perturbation of dead cells by swimming cells. The simple theory developed earlier predicts an exponential form for this part of the autocorrelation function, the decay constant of which exhibits no angle dependence but a linear concentration dependence. Evidence to support these two predictions is given in Figs. 3 and 4. In Fig. 3 the decay constant of the slow autocorrelation component is shown to be constant within experimental error over the restricted range of scattering angles used in these experiments. The decay

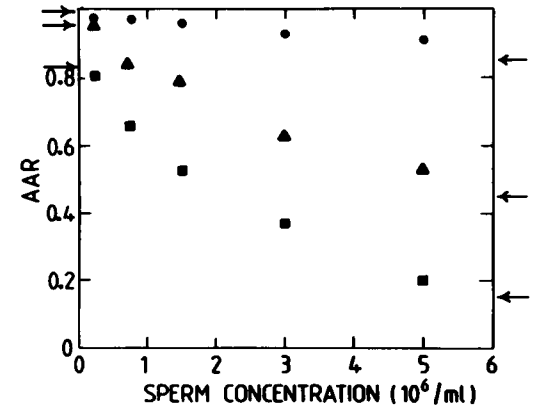

FIGURE 2 Dependence of the AAR on the total cell concentration with various proportions of motile cells as determined by a differential staining test: 85% dead (●), 45% dead (▲), and 15% dead (■). Arrows show the high and low concentration limits of the theory discussed in the text.

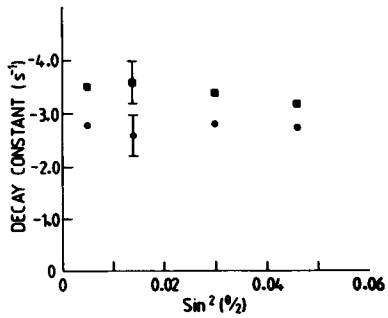

FIGURE 3 Dependence of the decay constant of the slow component of the composite autocorrelation function upon scattering angle, for light scattered from samples of bull spermatozoa from two different bulls (■ and ●). Typical error bars are shown for one angle.

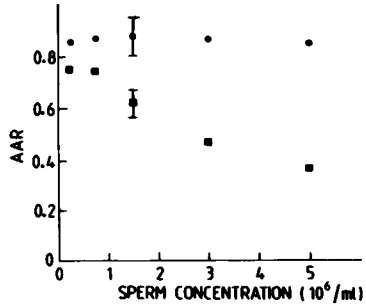

FIGURE 5 The dependence of the AAR on the total cell concentration at temperatures of 37°C (■) and 28°C (●). Typical error bars are shown at one concentration. For both of these curves the apparent proportion of dead cells as determined by a differential stain count immediately after collection was 18%. The curves at 37°C can be compared with those in Fig. 2.

constant does, however, depend on the particular sample: the data shown derived from samples from two different bulls, the more vigorously swimming motile cells leading to a faster decay constant for their associated immotile fraction. In Fig. 4 the decay time of the slow autocorrelation component is plotted against the concentration of motile cells and shows evidence of a linear dependence on this parameter. It may be noted that the data points in this figure derive from experiments over a range of total cell concentrations and proportions of dead cells (e.g., the two points at 4×10^6 cells/ml derive from experiments at total concentrations of 5×10^6 cells/ml with 20% dead and 10^7 cells/ml with 60% dead).

The variation of the AAR and of the decay time of the slow autocorrelation component with sperm concentration was also found to be temperature dependent. This dependence (shown in Fig. 5) can be explained in a similar fashion. No concentration dependence of the AAR was apparent at the lower temperature, but a similar curvilinear relationship to that of Fig. 2 was obtained at a higher temperature. This is further evidence for sperm interaction effects, because, although the sample still contained a substantial motile fraction at 28°C, this fraction was observed microscopically to be swimming with greatly reduced vigor and translational speed.

Further experiments showed that the addition to the diluent of bovine seminal plasma (<10%), which has the effect of increasing the swimming vigor, generally gave a decrease in AAR and an increase in the autocorrelation decay constant, suggestive of an increased interaction level. Other experiments in which dead cells were added to a fixed concentration of motile cells showed that the AAR increased steadily as a function of the percentage of dead cells, but that its absolute value depended upon the concentration of motile cells. The decay constant of the slow component however, was found to be independent of the percentage of dead cells for a fixed concentration of motile cells, as expected on the basis of the interaction model.

The involvement of optical orientational effects in generating the slow autocorrelation component was also apparent when comparing the functions obtained with both horizontal and vertical alignment of the photodetector at the same forward scattering angle (see Fig. 6). With vertical alignment the autocorrelation function reduced to a fast decaying strongly damped osillatory function with no slow component. In terms of the model discussed previously, this may be understood as indicating that the immotile fraction, through geotactic orientation, becomes invisible to a vertically aligned detector. With such alignment, the

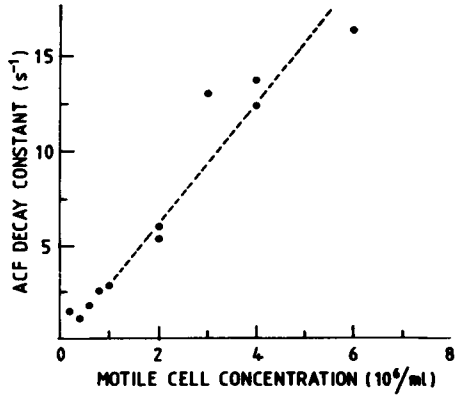

FIGURE 4 The dependence of the decay constant of the slow autocorrelation component upon the motile cell concentration. The dotted line is derived from the interaction model (see text).

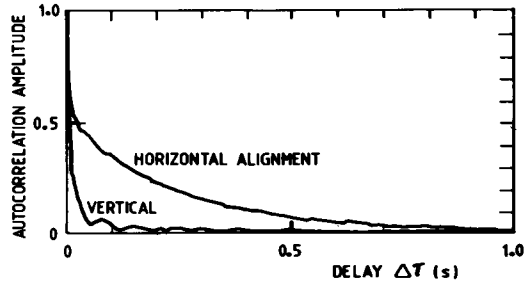

FIGURE 6 Autocorrelation functions obtained at a scattering angle of 8° for alignment of the photodetector in both the vertical and horizontal planes (k = 2.65 μm^{-1} sample concentration 10^6 cells/ml).

detector sees only the motile cells (~20%) that are swimming such that during head rotation the normal to the head plane becomes aligned within 20° of the scattering vector. The composite autocorrelation function in this case comprises a rapidly decaying component with a periodic feature generated by the multiple intensity peaks which occur during head rotations. Such features are well described by the predictions of Eq. 5 or the more complete calculation of Craig et al. (1979).

DISCUSSION

We undertook these experiments in an effort to understand the general features of the composite autocorrelation function generated by laser light scattering from a mixture of motile and immotile bull spermatozoa. The relative amplitudes of the two components of the autocorrelation function (having decay times differing by about two orders of magnitude at forward scattering angles) yield potentially valuable information concerning the relative number of motile and immotile cells. Detailed investigation has shown that various complex phenomena strongly affect the ratio of the amplitudes of the two components. On the basis of these experiments a simple theory has been developed to explain the dependence of the amplitude ratio of the two components upon the cell concentration. The approach adopted here has been to attempt to develop a qualitative understanding of the nature of the composite autocorrelation function of laser light scattered from mixtures of motile and immotile bull spermatozoa that is not sensitive to the details of the swimming or diffusing motion of the cells and is not based upon theoretical assumptions which may prove inadequate. The results presented here deal mainly with the form of the slow part of the composite autocorrelation function, which has not previously been stuided in detail, and can be understood on the basis of motile/immotile cell interactions, geotaxis of immotile cells, and wall-swimming behavior of motile cells.

The predictions of the interaction model for the form of the slow autocorrelation component are quite different from those of other models (such as a Brownian motion or a defective swimmers model) and are in substantial agreement with experiment. The results portrayed in Fig. 4 show that the decay constant of this part of the autocorrelation function is linearly dependent upon motile cell concentration. The slope of this graph can be related to the interaction radius of the dead cells. Neglecting wall-swimming effects and using Eq. 10 with an assumed mean swimming velocity of 150 μs^{-1} leads to an interaction radius of 80 μm. Cinematographic studies generally indicate an amplitude of motion of the flagellum of less than this (~15 → 20 μm), but the effective interaction range will be increased by the extended linear nature of the perturbed cells and the possibility of short range hydrodynamic coupling in addition to direct collisions. The interaction radius is an orientationally averaged cross-section for interactions between motile and immotile cells. Although the value indicated by the data is larger than the largest linear dimension of the spermatozoon, interactions over such distances are made more reasonable in the light of the very small perturbations necessary to inhibit the reflection of light from an immotile cell (a rotation of a few degrees about the axis of the flagellum is sufficient at typical scattering angles—such a perturbation would not be visible microscopically).

The interaction model we outline here also predicts no angle dependence of the decay rate of the slow component of the autocorrelation function. Although this prediction is upheld by the data of Fig. 3, it is not to be expected that this will hold over a much wider angular range than that investigated. In obtaining this simple prediction, two assumptions were made which can be expected to fail outside the angular range shown. At very small scattering angles (below 5°), the scattering lobe from the head of the spermatozoon increases in angular width (see Harvey and Woolford, 1980) and at angles of ~1°, the cells can no longer be considered as acting as mirrors. Changes in angular orientation at very low scattering angles, therefore, will not cause the scattered light intensity to change as dramatically as at larger scattering angles. This effect can be expected to increase the decay time of the slow component of the composite autocorrelation function at very small scattering angles. Some evidence for this was found in an experiment performed at a scattering angle of 4° where the decay constant of the slow component of a mixture dropped to a value of ~ 2 s^{-1} from a steady value of 3.5 s^{-1} over the range 8° → 25°. It should be noted however, that collisional effects still dominate the form of the function, since the decay constant of a totally immotile spermatozoa suspension at this angle (4°) was ~ 0.3 s^{-1}. Correlation functions with decay times of seconds are very difficult to measure accurately, however, because they involve data collection times of hours over which period the dead cells will sediment out of the sample volume.

At large scattering angles (>25°) the decay time of a totally immotile suspension becomes comparable with that of the slow component of a composite function, and is no longer reasonably approximated by a single exponential. Thus Eq. 7 no longer predicts a single exponential form for the slow component of a composite function. Furthermore, the mean intensity scattered from dead cells drops rapidly with increasing scattering angle and using the Rayleigh-Gans-Debye approximation the cells are found to no longer behave as thin mirrors because of destructive interference from opposite sides of the head. It is likely that at large angles, the relative contribution of scattering from the midpiece or flagellum of the cells becomes significant compared with that from the head, thus invalidating the simple approach outlined here.

In addition to the predictions concerning the decay constant of the slow component of the autocorrelation function, the interaction model was developed in an attempt to understand the form of the AAR versus concen-

tration curves which are typified by the results in Fig. 2. The prediction that the AAR will vary strongly with cell concentration over the concentration range $(0.5 \rightarrow 5) \times 10^6$/ml is supported by the curves of Fig. 2, and the limits at high and low concentration are in reasonable agreement with this theory. The limits are indicated by arrows on the graphs of AAR versus concentration in Fig. 2, and have been calculated from Eq. 11 and 12 using a value of $\gamma = 0.2$ and $W = 0.8$ for the zero concentration limit (values of W of this magnitude are consistent with our own microscope observations at low concentration), and $W = 0$ for the high concentration limit. Part of the variation of the AAR with cell concentration can be explained by motile/immotile cell interactions, which reduce the proportion of immotile cells in the visible head-down attitude. The dramatic dependence shown in Fig. 2, however, can only be explained by a combination of this effect, and a strong dependence of W upon concentration. Such a dependence is quite reasonable in view of the rapidly increasing frequency of motile cell collisions on the scattering cell walls as the concentration is increased. The functional form of this dependence, and the absolute value of W at a given concentration, however, also depend upon the geometry of the scattering cell (notably its surface to volume ratio) used in the experiments, and are difficult to model reliably.

Thus, although this theory can be developed further (Woolford, 1981), its quantitative predictions depend upon details of the interactions which are not yet available, and these developments will not be presented here. We consider that this problem is best approached by designing a new detection system for the scattered light which enables the detector to collect light from all cells independently of their orientation. Preliminary results using such a detection system have shown no concentration dependence of the AAR (Woolford, 1981).

A further point which should be considered is the possibility of a real dilution effect, in which the variation of the AAR is caused by immobilization of sperm as a result of dilution of the sample. Such effects have often been noted in the literature, but depend upon the diluent used and are probably attributable to dilution of the seminal plasma. We carried out experiments where seminal plasma was added back, after dilution of the spermatozoa and indeed some limited reactivation was often observed. Even in this type of study, however (with added seminal plasma), we observed the same concentration dependent effects described in this paper. We conclude, therefore, that while the possible contribution of a real dilution effect cannot be excluded, the major contributing factor to the dependence of the AAR on concentration is that of interactions with motile cells. One further possible influence on the amplitude ratio of the fast and slow components of the autocorrelation function concerns the contribution of diffusing contaminant particles. Samples of bull spermatozoa generally contain various levels of cellular contaminants. The proportion of such contaminants depends on the collection and processing techniques employed, and in cases of severe contamination, a component of the autocorrelation function generated by such debris must be included. In our experiments, the level of other scattering centers was found, by microscopy, to be very small, and we did not find it necessary to include such a component in the autocorrelation function analysis in order to explain our results. Evidence that the level of scattered light from such components was indeed negligible can be found in Fig. 6 where the slow component of the autocorrelation function is seen to become negligible for a vertically aligned detector. This indicates the absence of any significant contribution from large diffusing particles which scatter isotropically. Corrections, may, however, be necessary in cases where the level of contamination is greater.

In conclusion, our data provide strong evidence for an interaction model, in which the general form of the complete autocorrelation function of motile/immotile mixtures of bull spermatozoa is strongly affected by the disturbance of dead cells caused by the swimming cells. The details of this dependence are so complex, however, that no absolute measurement of the proportion of dead cells in the mixture can be made from the autocorrelation functions. Previous workers have developed extensive theoretical models to fit the fast decaying part of the autocorrelation function, but have found great variability in the amplitude and decay of the slow part of this function (e.g., Hallett et al., 1978). The reasons for this variability are clear on the basis of the work reported here. It should be noted, however, that even if the proportion of dead cells is not a parameter accessible to measurement by the normal laser light-scattering method, the fast decaying component gives useful information on the rotation rate of the swimming cells, and, as can be seen from Fig. 6, using the conventional detection system, this component is best studied using a vertically oriented detector, since in this case, the slowly decaying part of the function becomes negligible after geotactic relaxation of the dead cells at typical concentrations.

The authors express their appreciation of the resources, samples and assistance provided by Mr. P. Shannon and Mr. B. Curson of the New Zealand Dairy Board. The contributions and assistance of colleagues Dr. R. Sherlock of the University of Waikato, and Mr. D. S. M. Phillips and Mr. J. K. Woolhouse of the Ruakura Agricultural Research Centre are also gratefully acknowledged.

Received for publication 8 May 1981 and in revised form 12 May 1982.

REFERENCES

Chu, B. 1974. Laser Light Scattering. Academic Press, Inc., New York. 152–200.

Cummins, H. Z. 1977. Intensity fluctuation spectroscopy of motile microorganisms. *In* Photon Correlation Spectroscopy and Velocimetry. H. Z. Cummins and E. R. Pike, editors. Plenum Press, New York. 200–225.

Cooke, D. F., F. R. Hallett, and V. A. V. Barker. 1976. Motility

evaluation of bull spermatozoa by photon correlation spectroscopy. *J. Mechanochem. Cell Motil.* 3:219–223.

Craig, T., F. R. Hallett, and B. Nickel. 1979. Quasi-elastic light scattering spectra of swimming spermatozoa. *Biophys. J.* 28:457–472.

Hallett, F. R., T. Craig, and J. M. Marsh. 1978. Swimming speed distributions of bull spermatozoa as determined by quasi-elastic light scattering. *Biophys. J.* 21:203–212.

Harvey, J. D., and M. W. Woolford. 1980. Light scattering studies of bull spermatozoa. I. Orientational effects. *Biophys. J.* 31:147–156.

Katz, D. F., and J. R. Blake. 1974. Flagellar motions near walls. *In* Symposium on Swimming and Flying in Nature. T. Y. T. Wu, C. J. Brokaw, and C. Brennan, editors., Plenum Press, New York. 173–184.

Nossal, R. 1971. Spectral analysis of laser light scattered from motile micro-organisms. *Biophys. J.* 11:341–354.

Roberts, A. M. 1970. Motion of spermatozoa in fluid streams. *Nature* (*Lond.*). 228:375–376.

Roberts, A. M. 1972. Gravitational separation of X and Y spermatozoa. *Nature* (*Lond.*) 238:223–225.

Rothschild, Lord. 1963a. *In* Spermatozoan Motility. D. W. Bishop, editor, American Association for the Advancement of Science, Washington, D. C. 13–29.

Rothschild, Lord. 1963b. Non-random distribution of bull spermatozoa in a drop of sperm suspension. *Nature* (*Lond.*). 198:1221–1222.

Shannon, P. 1965. Contribution of seminal plasma, sperm numbers and gas phase to dilution effects of bovine spermatozoa. *J. Dairy Sci.* 55:1–7.

Shannon, P. 1973. Factors affecting storage of semen. *Proc. N. Z. Soc. Anim. Prod.* 33:40–48.

van Duijn, C., Jr. 1973. Positive hydrodynamic interaction between swimming bull spermatozoa. *Ann. Biol. Anim. Biochim. Biophys.* 13:7–15.

Walton, A. 1952. Flow orientation as a possible explanation of 'wave-motion' and 'rheotaxis' of spermatozoa. *J. Exp. Biol.* 29:520–531.

Woolford, M. W. 1981. Laser light scattering as a proble of bovine sperm motility. PhD Thesis. University of Waikato, New Zealand.